

Multi-Image Deblurring using Complementary Sets of Fluttering Patterns

Hae-Gon Jeon, *Student Member, IEEE*, Joon-Young Lee, *Member, IEEE*, Yudeog Han,
Seon Joo Kim, *Member, IEEE*, and In So Kweon, *Member, IEEE*

Abstract—We present a novel coded exposure video technique for multi-image motion deblurring. The key idea of our work is to capture video frames with a set of complementary fluttering patterns, which enables us to preserve all spectrum bands of a latent image and recover a sharp latent image. To achieve this, we introduce an algorithm for generating a complementary set of binary sequences based on the modern communication theory and implement the coded exposure video system with an off-the-shelf machine vision camera. To demonstrate the effectiveness of our method, we provide in-depth analyses of the theoretical bounds and the spectral gains of our method and other state-of-the-art computational imaging approaches. We further show deblurring results on various challenging examples with quantitative and qualitative comparisons to other computational image capturing methods used for image deblurring, and show how our method can be applied for protecting privacy in videos.

Index Terms—Image deblurring, computational photography, coded exposure, video privacy protection.

I. INTRODUCTION

IMAGE deblurring is a classic computer vision problem that has been researched for a long time and yet no clear cut solution exists due to its ill-posedness. To solve this ill-posed problem, most of the solutions employ a type of optimization scheme with some prior knowledge. While much progress has been made recently, restoring heavily blurred images is still a very challenging problem where previous methods tend to output over-smoothed images. This is because the conventional camera exposure process acts as a box filter, destroying important spatial details of latent images.

A promising solution to the problem is the coded exposure imaging [1], which is a computational imaging system that captures an image by fluttering a camera’s shutter open and close in a special manner within the given exposure time. This approach modulates the integration pattern of light, and it enable us to capture an image with invertible motion blur

We thank for Tae Hyun Kim and Jinshan Pan generating comparison images. This work was supported by the National Research Foundation of Korea(NRF) grant funded by the Korea government(MSIP) (No.2010-0028680). Hae-Gon Jeon was partially supported by Global PH.D Fellowship Program through the National Research Foundation of Korea(NRF) funded by the Ministry of Education (NRF-20151034617).

H.-G. Jeon is with the School of Electrical Engineering, KAIST, Daejeon, Korea. (e-mail : hgjeon@rcv.kaist.ac.kr)

J.-Y. Lee is with Adobe Research, San Jose, USA.

Y. Han is with Agency for Defense Development, Daejeon, Korea.

S.J. Kim is with the Department of Computer Science, Yonsei University, Seoul, Korea. (e-mail : seonjookim@yonsei.ac.kr)

I.S. Kweon is a corresponding author of this paper and with the School of Electrical Engineering, KAIST, Daejeon, Korea. (e-mail : iskweon@kaist.ac.kr)

where frequency magnitude of point spread functions (PSF) is greater than zeros for all spectral bands. With the coded exposure imaging, therefore, we can recover a sharp latent image as this imaging method preserves lots of spectral bands in the blurred image. Recent studies in [2], [3] demonstrated that well-designed fluttering patterns suppress deconvolution noise of recovered images as well as preserve sharp edges. The coded exposure imaging has received much attention leading up to applications in various areas such as iris recognition [4], barcode scanning [5], and microscopy [6], [7].

One of limitations for coded exposure is losing incoming light compared to a traditional camera, which results in decreasing SNR of a latent image. The spectral gain is a measure to compute flatness of frequency response of fluttering patterns, and it reflects a mean square error of deblurred images. According to [8], a spectral gain of coded exposure is slightly more than half of that of the best snapshot. It means that there is still a room for improvement in coded exposure in terms of both amount of incoming light and the spectral gain of fluttering patterns.

Another interesting direction for image deblurring is to use multiple images. In [9], [10], two deblurring/denoising configurations were analyzed in depth; multiple sharp images with high-level noise captured using a short exposure time and a blurry but low-noise image using a long exposure time. Their analyses come to the conclusion that aligning-and-averaging multiple sharp but noisy images achieves higher SNR than deblurring a single image. The idea was later extended in [11], which showed that a better strategy is to capture a series of images with relatively small degree of blur using an intermediate exposure time and then recover a latent image by jointly deconvolving them.

In [12], Agrawal *et al.* proposed a video capturing strategy for the multi-image deblurring that changes the exposure time at each frame. This work achieved the automatic deblurring including the PSF invertibility, the PSFs estimation, and the moving object segmentation from a static background. However, this work amplifies the deconvolution noise by 4~5 dB compared to the coded exposure imaging [1].

In this paper, we propose a coded exposure video scheme which combines the advantages of both the coded exposure imaging [1], [2] and the varying exposure video [12]¹. Instead of varying the exposures between frames, we capture a video with a fixed exposure per frame and apply the coded

¹This paper extends [13] with deeper analysis on the benefit of the new capture strategy, further technical details of our implementations, and additional experiments and evaluations

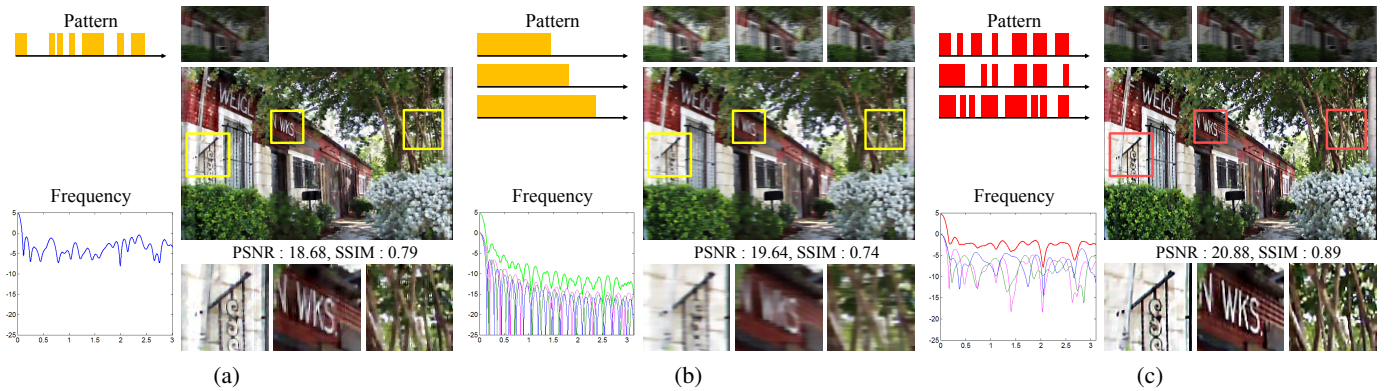


Fig. 1. Comparisons of different computational imaging techniques for image deblurring. (a) Coded exposure imaging [1]. (b) Varying exposure video [12]. (c) Proposed coded exposure video.

exposure scheme on every frame (Fig. 1(c)). To minimize the information loss during the image capture, we introduce the concept of complementary sets of fluttering patterns and show its theoretical optimal bounds in terms of the spectral gain and the magnitude of autocorrelation (Sec. III). We realize this concept by implementing the coded exposure video using an off-the-shelf machine vision camera (Sec. IV-A), and introduce a method for generating the complementary set of fluttering patterns (Sec. IV-B). In Sec. IV-C, we present a multi-image deblurring procedure to recover a sharp latent image from blurred images captured using our method. By using the complementary sets of fluttering patterns, we can generate various exposure time sequences for the flexible frame rate capture and also achieve higher quality deblurring results with improved SNR compared to the previous methods (Sec. V). We additionally show that our framework can be applied to other applications such as the privacy protection for video surveillance by adding intentional blurs [14] (Sec. VI).

II. RELATED WORKS

Image deblurring is a challenging task that is inherently an ill-posed problem due to the loss of high-frequency information during the imaging process. In the past decade, there have been significant developments in the image deblurring research that improve the performance over the traditional deblurring solutions such as Richardson-Lucy [15], [16] and Wiener filter [17].

One research direction that has gained interest is to use multiple blurred images for the deblurring, which shows better performance over the single image deblurring methods in general due to the complementary information provided. Yuan *et al.* used a blurry and noisy image pair to estimate the blur kernel [18], Cai *et al.* proposed to use multiple severely motion-blurred images [19], and Chen *et al.* performed an iterative blur kernel estimation and a dual image deblurring [20]. Cho *et al.* [21] presented a video deblurring approach that uses sharp regions in a frame to restore blurry regions of the same content in nearby frames. Delbracio and Sapiro [22] captured blurred image sequences and recovered a latent image by performing a weighted average of the images in the frequency domain where the weights are determined by the Fourier spectrum magnitude. In [23], [24], motion blur in

a video is reduced by increasing the frame-rate for temporal super-resolution.

Another research direction of image deblurring is to design hardware systems to minimize motion blur during exposure or to make the deblurring problem more feasible. Optical and electrical image stabilizer [25], [26] are used to reduce image blur associated with the motion of a camera by compensating rotation and translation of imaging devices. However, the stabilizer systems work for limited cases such as small motion from hand shaking. In order to handle larger image blur for surveillance and manufacturing inspection systems, specialized camera devices are designed in [27], [28], [29]. The systems capture a video whose each pixel is independently modulated by binary patterns, which enables the recovery of high temporal resolution.

On the other hand, this paper is particularly related to the works that employ imaging systems that control the exposures for the whole image, not on the pixel level, during image captures. This approach handles large motion blur effectively by only using an off-the-shelf camera. In [1], Raskar *et al.* presented the coded exposure photography that flutters the camera's shutter open and closed in a special manner within the exposure time in order to preserve the spatial frequency details, thereby enabling the deconvolution problem to become well-posed (Fig. 1(a)). Jeon *et al.* [2] improved the deconvolution performance by computing the optimized fluttering patterns. In [30], McCloskey replaced the flutter shutter with a temporal coded illumination. The coded illumination works by controlling a flash light array at low-light conditions for capturing fast moving objects and enables the recovery of a sharp appearance of the moving objects.

The coded exposure method has been recently applied to various areas. In [4] and [5], the coded exposure framework has been applied for the recovery of sharp iris images and 2D barcode images. Similar to [30], Ma *et al.* [7] proposed a LED array microscope with a controllable illumination. This approach generated a continuous illumination pattern and retrieved deblurred samples with high SNR. Gorthi *et al.* [6] designed a fluorescence microscope that controls the excitation light and captures flowing cells with a global shutter camera.

Instead of the fluttering shutter within a single exposure, Agrawal *et al.* [12] proposed a varying exposure video

framework which varies the exposure time of successive frames (Fig. 1(b)). The main idea is to image the same object with varying PSFs by varying the exposures so that the nulls in the frequency component of one frame can be filled with other frames, making the deblurring problem well-posed. Holloway *et al.* [31] applied the concept of coded exposure into a video camera. This approach captures a series of coded exposure images with different fluttering patterns in successive frames and performs temporal resolution upsampling via compressed sensing. As mentioned in [31], this approach cannot handle scenes without the spatiotemporal continuity and requires many observations for estimating the object motion.

In the coded exposure imaging, designing the fluttering pattern is crucial in determining the performance of the image restoration. Raskar *et al.* [1] computed the fluttering patterns via a random sample search and used the minimum spectrum of a fluttering pattern as the objective function. McCloskey *et al.* [3] also presented a search-based method that incorporates natural image statistics in generating fluttering patterns. However, those measures may fail to generate consistently good fluttering patterns when the size of the patterns becomes long or images do not follow the natural image statistics.

To deal with the problem, Jeon *et al.* [32] showed that the magnitude of the autocorrelation of binary sequences in the frequency domain is a good measure of a fluttering pattern and presented a principled way for designing the fluttering patterns. Following the development of [12], [2], we introduce a new concept of video capturing for multi-image deblurring in this paper. In our framework, different fluttering patterns that are computed using complementary sets of sequences are applied at each frame allowing for the sharp recovery of latent images. We assume the velocity of an object is unchanged during taking an image and focus on handling linear motion blur.

III. COMPLEMENTARY SET OF SEQUENCES AND CODED EXPOSURE

The key idea of this paper is to capture video frames with a set of fluttering patterns that compensate frequency losses in each frame, so that the captured images preserve spatial frequencies. To generate such fluttering patterns, we introduce the *complementary set* of binary sequences [33], which have been widely used in many engineering applications such as the multiple-input-multiple-output (MIMO) radar [34], the code division multiple access (CDMA) technique [35], infrared spectrometry [33], and radar [34]. In this section, we theoretically show the advantage of the coded exposure video with the complementary set of fluttering patterns over the coded exposure imaging [1], [2] and the varying exposure video [12].

A. Coded Exposure Imaging vs. Coded Exposure Video

In [1], it has been shown that a fluttering pattern with a flat spectrum improves the quality of the deblurring in the coded exposure imaging. To measure the flatness, they use the sum of an autocovariance function of a fluttering pattern. It is

also shown in [2] that an autocorrelation function of a binary sequence can be approximated by an autocovariance function. With a binary sequence $U = [u_1, \dots, u_n]$ of length n , the relationship between the autocorrelation and the modulated transfer function (MTF : a magnitude of frequency response of binary sequence) via the Fourier transform of the sequence is derived as ([36])

$$\sum_{k=1}^{n-1} \Psi_k^2 = \frac{1}{2} \int_{-\pi}^{\pi} [|\mathcal{F}(U)|^2 - n]^2 d\theta, \quad (1)$$

where $\mathcal{F}(U)$ represents the Fourier transform of the sequence U , and θ is an angular frequency. Ψ_k denotes k^{th} element of the autocorrelation function Ψ of the sequence, which is defined as

$$\Psi_k = \sum_{j=1}^{n-k} u_j u_{j+k}. \quad (2)$$

In [2], it is shown that a smaller value of Eq. (1) reflects higher merit factor, which in turn results in better deblurring performance. Ukil proves in [37] that the minimum value of Eq. (1) is bounded by $n/2$.

In our coded exposure video framework, a complementary set is defined as a set of binary sequences where the sum of autocorrelation functions of the sequences in the set is zero. If we have a complementary set Δ consisting of $p (\geq 2)$ sequences $\{U_1, \dots, U_p\}$ of length n , the relationship is denoted as

$$\sum_{i=1}^p \Psi_k^i = 0 \quad \text{for any } k \text{ except } k \neq 0, \quad (3)$$

where Ψ_k^i denotes k^{th} element of the autocorrelation function Ψ of the i^{th} sequence in Δ .

It is shown in [38] that a complementary set Δ is computed by minimizing

$$\sum_{k=1}^{n-1} \left| \sum_{i=1}^p \Psi_k^i \right|^2 = \frac{1}{2} \int_{-\pi}^{\pi} \left[\sum_{i=1}^p |\mathcal{F}(U_i)|^2 - pn \right]^2 d\theta. \quad (4)$$

In the optimal case, the minimum value of Eq. (4) becomes zero from Eq. (3). This means that the joint spectrum of a complementary set has flatter spectrum than that of a single binary sequence (coded exposure imaging) since Eq. (1) is bounded to $n/2$ for a single binary sequence as mentioned above.

B. Performance Invariance to Object Velocity

When the object moves over a range of n pixels during a shot, the optimal length of a fluttering pattern $U = [u_1, \dots, u_n]$ is n . As demonstrated in [39], if the object moves twice as fast, the effective PSF is stretched $\frac{1}{2n}[u_1, u_1, \dots, u_n, u_n]$ and the invertibility of the PSF cannot be guaranteed.

We show that complementary set of sequences minimizes the loss of spectral information even when the effective PSFs are super-sampled or stretched due to the velocity of an object. As an example, we derive the change of MTF due to a stretched sequence by a factor 2:

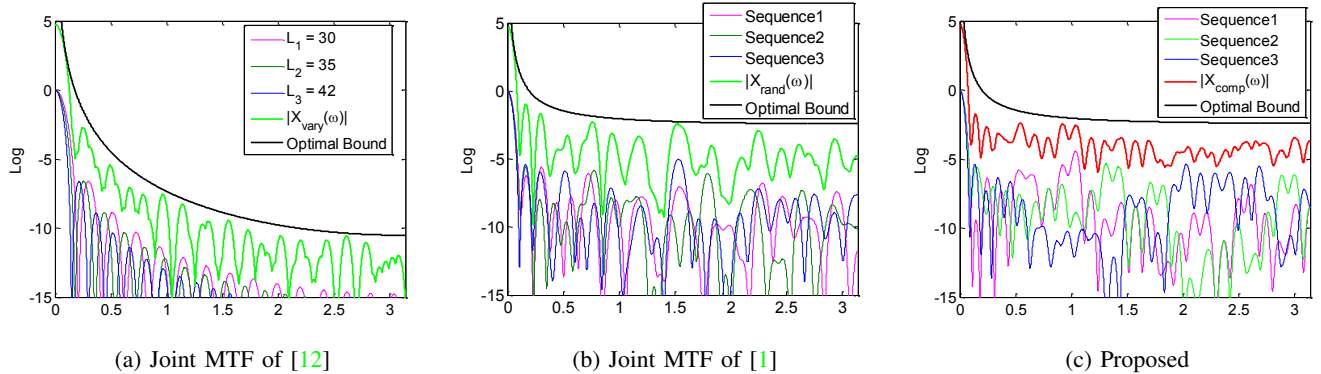


Fig. 2. Joint MTF of each method and its theoretical upper bound. (a) Varying exposure video [12]. (b) Different fluttering patterns by random sample search [1]. (c) The proposed method by complementary set of fluttering patterns.

$$\begin{aligned}
b_i &= \sum_{j=0}^{2n-i-1} U_{2n}U_{2n}(j+i) \\
&= \sum_{p=0}^{n-q-1} [U_{2n}(2p)U_{2n}(2p+2q) + U_{2n}(2p+1)U_{2n}(2p+2q+1)] \\
&= \sum_{p=0}^{n-q-1} [U_n(p)U_n(p+q) + U_n(p)U_n(p+q)] = 2\Psi_q,
\end{aligned}$$

where $j = 2p$ and $i = 2q.$ (5)

The variance of the MTF of the stretched PSF is constant times bigger than the PSF as follows:

$$\sum_{i=1}^{n-1} b_i = 4 \sum_{k=1}^{n-1} \Psi_k^2 = 2 \int_{-\pi}^{\pi} [|\mathcal{F}(U_n)|^2 - n]^2 d\theta. \quad (6)$$

As mentioned in Sec. III-A, the optimal bound of $\frac{1}{2} \int_0^1 [\mathcal{F}(U_n) - n] d\theta$ in the complementary set of sequences is theoretically zero. Thus, the optimal bound of the decimated PSF also becomes zero. In practice, because our set of sequences is close to the optimal bound, the proposed complementary set can handle the velocity dependency issue and it can be shown for the case of any factor. Our system's robustness to the object velocity is also demonstrated in the Experiments Section.

C. Varying Exposure Video vs. Coded Exposure Video

To compare our coded exposure video framework with the varying exposure video [12], we analyze the upper bound of MTFs for these two methods. The main criteria for the comparisons are the variance, the minimum, and the mean of the MTF. As shown in [1], [3], the MTF of a binary sequence in the coded exposure photography has a direct impact on the performance of the image deblurring. The variance and the mean of the MTF are related to deconvolution noise, and the peakiness of the spectrum has an ill effect on deblurring since it destroys the spatial frequencies in the blurred image.

The MTF of the varying exposure method [12] is the joint spectrum of different durations of rectangle functions in the

time domain (Fig. 2(a)). The upper bound of the joint MTF X_{vary} of p varying exposures is derived as

$$|X_{vary}(\omega)| = \sum_{i=1}^p |\mathcal{F}(\Pi(l_i))| = \sum_{i=1}^p \left| \frac{\sin \frac{l_i}{\omega} \omega}{\sin \frac{\omega}{2}} \right| \leq \left| \frac{p}{\sin \frac{\omega}{2}} \right|, \quad (7)$$

where $\Pi(l)$ denotes a rectangle function of length l , and ω is a circular frequency at $[-\pi, \pi]$.

To compute the upper bound for the coded exposure video, let Φ denote a binary sequence of $+1$'s and -1 's. Parker *et al.* [40] showed that the sum of all the Fourier transform components of a complementary set of p sequences $\Phi_i, i = [1, \dots, p]$ of length n is at most \sqrt{pn} . Since a fluttering pattern in the coded exposure imaging is made of $+1$'s and 0 's due to its physical nature, the upper bound of the joint MTF X_{comp} of a complementary set is computed as

$$\begin{aligned} |X_{comp}(\omega)| &= \frac{1}{2} \sum_{i=1}^p |\mathcal{F}(\Phi_i + \Pi(n))| \\ &\leq \frac{1}{2} \sum_{i=1}^p |\mathcal{F}(\Phi_i)| + \frac{1}{2} \sum_{i=1}^p |\mathcal{F}(\Pi(n))| \leq \frac{1}{2} \sqrt{pn} + \left| \frac{p}{2 \sin \frac{\omega}{2}} \right|. \end{aligned} \quad (8)$$

Fig. 2 compares the joint MTF of the varying exposure video and the coded exposure video with the theoretical upper bound in Eq. (7) and Eq. (8). For the varying exposure video in (a), the exposure lengths of [30, 35, 42] are used as in [12]. For the coded exposure video, we use three random sequences from [1] in (b) and our complementary set of binary sequences in (c) which will be explained in the next section. As can be seen in the figure, no null frequency is observed at the MTFs of each coded pattern in the complementary set. This means that each single frame becomes invertible as with the conventional coded exposure imaging [1], [2]. In (b), the peaky spectrums of the random binary sequences are moderated but the variance of the joint MTF is still large. The peaky spectrums of each sequence in the complementary set are well compensated by the joint MTF (c), and the joint MTF (c) has much flatter and higher MTF than the joint MTFs of both the varying exposure method (a) and the set of the random sample sequences (b).

Theoretical upper bounds as well as the actual performance measurements of the MTF properties for the varying exposure video and the coded exposure video are plotted in Fig. 3.

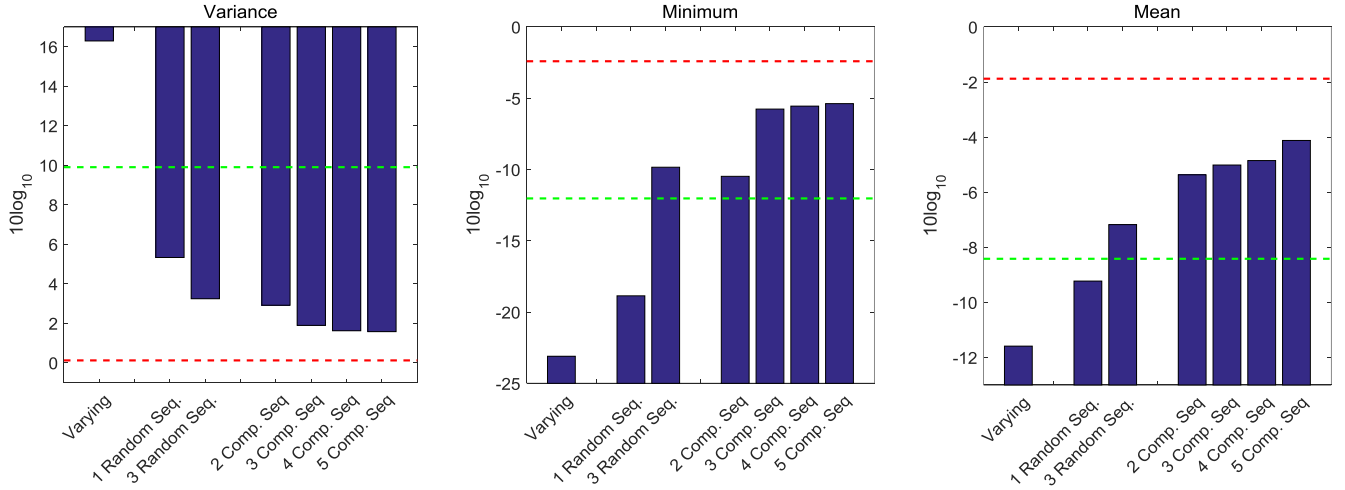


Fig. 3. The theoretical upper bound and the actual performance measurement of the varying exposure video and the coded exposure video in terms of MTF properties. Green lines and red lines represent theoretical optimal bounds of the varying exposure video and the coded exposure video, respectively.

TABLE I
SPECTRAL GAINS OF DIFFERENT COMPUTATIONAL IMAGING METHODS FOR MOTION DEBLURRING.

Method	Spectral Gain
Single Coded Exposure [1]	0.5636
Varying Exposure [12]	0.5782
Three Different Patterns	0.6581
Proposed (3 Patterns)	0.7730~0.8331
Proposed (4 Patterns)	0.8554

To verify the effectiveness of the complementary set of fluttering patterns, the random sample search method in [1] is used to generate the binary sequences for single image and three images cases. Although the MTFs of both the coded exposure and the varying exposure do not reach the lower (variance) and the upper bound (mean and minimum), the coded exposure patterns show better MTF properties than both the varying exposure method and the set of random sequences. Specifically, the complementary set has a jointly flat spectrum with higher mean and minimum MTF value which are even better than the theoretical bounds of the varying exposure method. This shows that the complementary set preserves spatial frequencies well by compensating frequency losses in each frame. It is worth noting that while utilizing all the sequences in a complementary set is ideal in theory, utilizing a partial set of the complementary set is also effective as shown in Fig. 2 and Fig. 3.

D. Spectral Gain

According to the work in [8], we estimate the spectral gain of the complementary set of sequences over an optimal snapshot to quantitatively analyze the performance gain of our method. Tendero *et al.* [8] have proven that the energy function of fluttering patterns in the frequency domain is denoted as:

$$G(U) = \frac{1}{2\pi\sqrt{v}} \frac{\int_{-\pi}^{\pi} |\mathcal{F}(U)| d\theta}{\sqrt{\|U\|_1}}, \quad (9)$$

where v is velocity of a moving object and $\|\cdot\|_1$ is the L_1 norm. $G(U)$ represents integral of a normalized MTF of a PSF $\mathcal{F}(U)$. Because we are only interested in the numerical gain of fluttering patterns, we set v to 1 in Eq. (9). To maximize the $G(U)$, Fourier transform of fluttering patterns should be constant. Then, the spectral gain is obtained by the ratio of two energies between the optimal snapshot² and the target imaging method.

We estimate spectral gains of different capturing methods with the same exposure time. The result is summarized in Table I. The spectral gain of our complementary set consisting of 4 sequences is 0.8554. The gain of 3 selected sequences from the set is 0.7730~0.8331, which is much higher than the spectral gains (0.56 and 0.57) of the single coded exposure method [1] and the varying exposure method [12].

In [8], they also proposed the concept of a “continuous numerical flutter shutter”, and showed that the sinc function whose spectrum is completely flat is the best fluttering pattern (spectral gain: 1.17). Although our complementary set consists of binary sequences, its joint form is similar to that of the numerical shutter. We observed that the spectral gain is directly proportional to the PSNR and SSIM values through our synthetic experiments Sec. V-A.

IV. CODED EXPOSURE VIDEO

A. Implementation of Coded Exposure Video

Constructing a hardware system for the coded exposure video is not trivial. We implemented the coded exposure video system using a Point Grey Flea3 GigE camera which supports the multiple exposure pulse-width mode (Trigger Mode 5) and an ATmega128 microcontroller to generate external trigger pulses as shown in Fig. 4 (a). In the multiple exposure pulse-width mode, the shutter time is controlled by the width of a trigger pulse generated by the microcontroller. Data transfer between the computer and the camera is done

²In [8], the energy G of the optimal snapshot is 0.1359. We use this value for computing spectral gains.

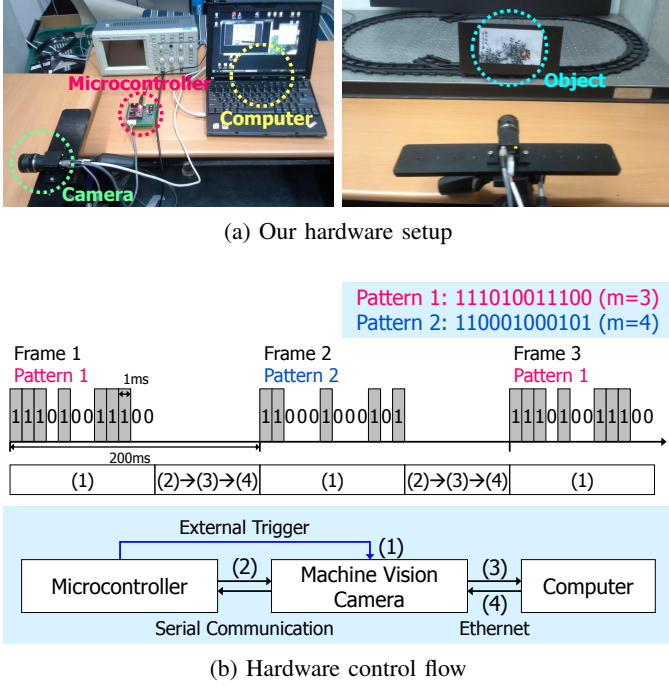


Fig. 4. Hardware Setup for the Coded Exposure Video.

through Ethernet and the messages are delivered using the serial communication. Messages are sent to the microcontroller from the computer, which includes a set of fluttering patterns and two signals indicating the start and the end of the image capture.

Fig. 4 (b) shows the overview of our coded exposure video implementation. The camera finishes taking an image after c times of peaks in a trigger signal (gray area in the figure), which indicates the end of a sequence (step 2). Then, the camera transmits a recorded image and an end signal to the computer (step 3), and the computer passes the parameter c of the next sequence to the camera (step 4). We used this system to capture both varying exposure videos and coded exposure videos. Each shutter chop is 1ms long and the frame rate is fixed to 5 frames per second regardless of the sequence length due to our hardware limitation. The implementation manual and the source code of this capture system are released on our project page, https://sites.google.com/site/hgjeoncv/complementary_sets/.

B. Generating Complementary Sets of Fluttering Patterns

In the coded exposure imaging, a fluttering pattern of a camera shutter generally consists of a sequence longer than 20 bits, or even longer than 100 bits. Since the length of the fluttering pattern may vary due to the illumination condition or the object motion, it is beneficial to have a flexibility in the length of the pattern. In this subsection, we introduce a method for generating a complementary set of fluttering patterns of flexible length.

Our strategy for obtaining the flexibility in the sequence length is to generate the complementary set by expanding a small-sized initial set that is known to be a complementary set.

Since the research in the complementary set construction has a long history, many known complementary sets exist such as

$$\Delta = \begin{bmatrix} 0 & 1 \\ 0 & 0 \end{bmatrix}, \begin{bmatrix} 11101101 \\ 11100010 \end{bmatrix}, \begin{bmatrix} 000010100100 \\ 001001111101 \\ 101000100011 \\ 001110010111 \end{bmatrix},$$

where Δ denotes a complementary set in a matrix form. In Δ , each row vector represents one sequence and the set of all row vectors is a complementary set.

From an initial complementary set $\Delta_{(p,n)}$ which consists of p sequences of length n , we can iteratively generate larger complementary sets [33]. With a complementary set Δ , a new complementary set Δ^1 with larger length sequence is obtained by

$$\Delta^1 = \begin{bmatrix} \Delta & \Delta & \bar{\Delta} & \Delta \\ \bar{\Delta} & \Delta & \Delta & \Delta \end{bmatrix}, \quad (10)$$

where $\bar{\Delta}$ denotes the matrix with all the elements δ s in Δ flipped. After applying the expansion t times, we obtain a complementary matrix $\Delta^t \in \mathbb{R}^{2^t p \times 4^t n}$, which contains $2^t p$ sequences of length $4^t n$.

Another option for generating variable length sequences is to divide Δ into two matrices with the same length as

$$\Delta = [\Delta_L \ \Delta_R]. \quad (11)$$

In this case, both matrices Δ_L and Δ_R become complementary sets [41].

With the two matrix operations in Eq. (10) and Eq. (11), we can generate a complementary set, whose size is $2^t p \times 2^{2t} n$ or $2^t p \times 2^{2t-1} n$. Since there are many well-known initial complementary sets with various sizes, we can generate complementary sets with huge flexibility of sequence length using the two methods.

Fig. 5(a) shows an example of the joint MTF of a complementary set Δ . Fig. 5(b) and (c) are the joint MTFs after the operation in Eq. (11), respectively. In this case, Δ_L and Δ_R have the same spectrum because Δ is generated from Eq. (10) that expands a complementary set without the loss of the skew symmetric property of binary sequences.

In the video deblurring scenario, the required number of sequences (or images) are usually limited to 2~5 because it is enough to compensate for the frequency losses and taking many pictures may create additional problems such as the alignment and the field-of-view issue. Therefore, we first generate a complementary set that fits with the required sequence length, and then select the required number of sequences among many candidate sequences in the set.

As for the criteria for selecting sequences from the available set of sequences, we consider the number of open chops. In general, the generated sequences have similar number of open chops, e.g. $n/2$, however it could be slightly different especially for short length sequences. In this case, selecting sequences with equal number of open chops can be an important criterion to avoid flickering between frames.

To illustrate the performance difference with varying selection of candidate sequences, we generated a complementary set of fluttering patterns containing eight sequences and chose two

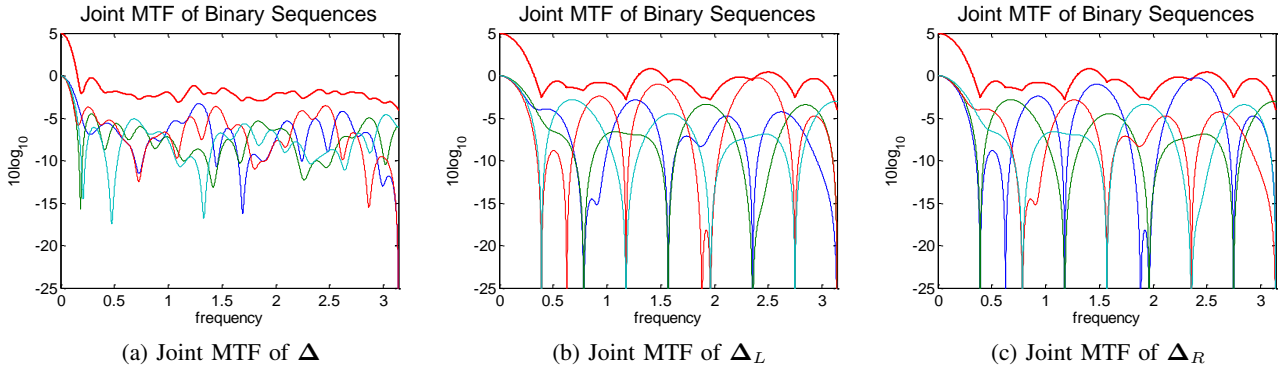


Fig. 5. An example of the joint MTF of a complementary set.

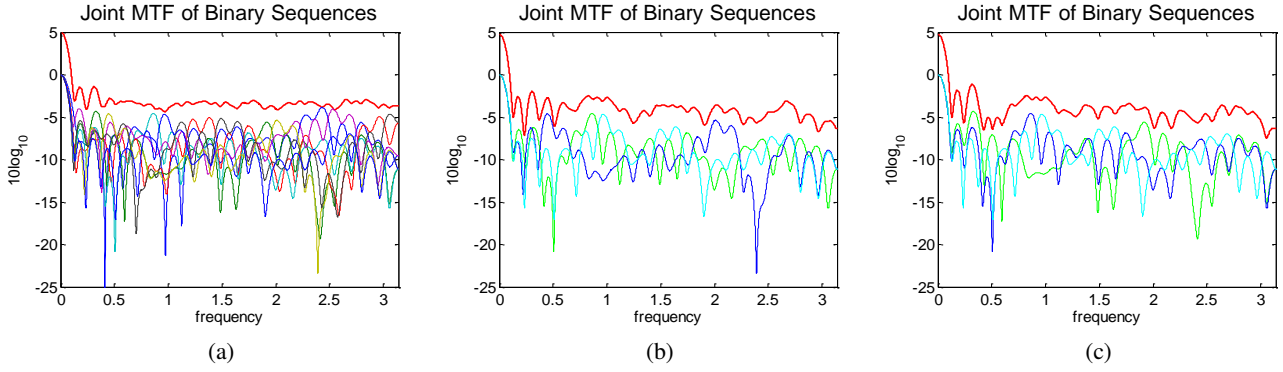


Fig. 6. Joint MTFs of the subsets of a complementary set. (a) joint MTF of a complementary set of fluttering patterns. (b,c) Joint MTFs of two different subsets consisting of three sequences.

different subsets consisting of three sequences. Fig. 6 shows the joint MTFs of both the complementary set and the subsets. Although the MTF properties of the subsets are slightly worse than that of the eight complementary set, the subset sequences still preserve the flat spectrum.

C. A Blurred Object Extraction and Deblurring

One practical issue with the coded exposure imaging is to extract an accurate matte image for the moving object deblurring. It is challenging because a blur profile becomes locally non-smooth due to the exposure fluttering. Agrawal and Xu [42] proposed the fluttering pattern design rules that minimize the transitions and maximize continuous open chops and showed that both criteria of PSF estimation [43] and invertibility can be achieved. In [44], a blurred object is extracted from a static background with user strokes in order to estimate motion paths and magnitudes. McCloskey *et al.* [3] presented a PSF estimation algorithm for coded exposure assuming that the image only contains a motion blurred object. In this paper, we deal with this matting issue by jointly estimating the PSF, object matting, and the multi-image deblurring. We assume that the images are captured from a static camera and a moving object is blurred by a constant velocity 1-D motion.

1) Initialization: To accurately extract the blurred object (Fig. 7(a)), we first capture background images and model each pixel of the background using a Gaussian mixture model (GMM). When an object passes over the background, we estimate an initial foreground layer by computing the Mahalanobis

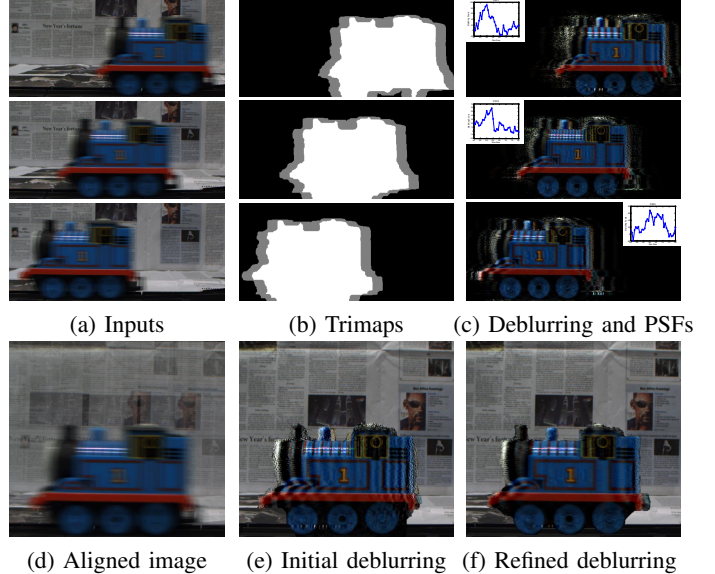


Fig. 7. Multi-image Deblurring Procedure

distance between pixels of each image and the background model. Since the estimated layers are somewhat noisy, we refine the layers by applying morphological operations and make trimaps. Using the trimaps (Fig. 7(b)), we extract the blurred object at each image via the closed form matting [45].

After the object matting, we estimate the PSF of each image based on the method in [3], which can handle the cases of

constant velocity, constant acceleration, and harmonic motion. Specifically, we first perform the radon transform and choose the direction with the maximal variance as a blur direction. This is because high spatial frequencies of a blurred image are collapsed according to a blur direction. Then, we compute matching scores between the power spectral density of the blurred image and the MTF of the fluttering pattern for various blur size. We determine the size of blur by choosing the highest matching score. With this method, we estimate the blur kernel of each coded blurred image independently (Fig. 7(c)). This is useful because we do not suffer from the violation of the constant motion assumption between frames that often occurs in practice.

With the estimated PSFs, the captured images are deblurred independently. Then, we align all images by an affine matrix of the deblurred images using SIFT feature matching [46], and merge all the captured images along with the alpha maps (Fig. 7(d)). In the merging step, we assume that the camera response function [47] is linear as we used a machine vision camera, and align the intensity level of all frames to the brightest frame using the exposure time of each frame.

2) Iterative Refinement: After the initialization, we iteratively optimize between a latent image and the segmentation masks. Based on the merged image with the PSFs, we perform a non-blind multi-image deblurring by minimizing the following energy term:

$$\operatorname{argmin}_Y \sum_{j=1}^m \|B_j - K_j Y\|^2 + \lambda_d \|\nabla Y\|^\rho, \quad (12)$$

where Y is a latent deblurred image, ∇Y is the gradient of the latent image, B_j is a set of linearly blurred images captured by a set of PSF matrices K_j . λ_d is the smoothness weight and m is the number of images. Since the background of each blurred image is already subtracted in B_j , we ignore artifacts from the background during this deblurring process. We set $\rho = 0.8$ for image deblurring [48] and $\rho = 0.5$ for the merged alpha map deblurring $\bar{\alpha}$ according to [44]. The deblurred alpha map $\bar{\alpha}$ is re-blurred to obtain a guidance alpha map $\hat{\alpha}$ which is incorporated as a soft constraint in the close form matting to refine the alpha map α for the moving object [49]:

$$\operatorname{argmin}_\alpha \alpha^T \mathbf{L} \alpha + \lambda_m (\alpha - \hat{\alpha})^T \mathbf{D} (\alpha - \hat{\alpha}), \quad (13)$$

where \mathbf{L} is the Laplacian matrix of the closed form matting, \mathbf{D} is a diagonal matrix and λ_m is the weight for the soft constraint.

With the refined alpha maps, we optimize the set of affine matrices \mathbf{H} that minimizes the energy function similar to the stereo matching as follows:

$$\begin{aligned} \operatorname{argmin}_{\mathbf{H}} \sum_{j=1}^{m-1} & \{ \lambda_a \min(|X_{ref} - H_j X_j|, \tau_{color}) \\ & + (1 - \lambda_a) \min(|\nabla X_{ref} - \nabla(H_j X_j)|, \tau_{grad}) \}, \quad (14) \end{aligned}$$

where X is independently deblurred image and X_{ref} is the reference view. λ_a balances the color and the gradient terms, and $\tau_{color}, \tau_{grad}$ are truncation values to account for outliers correspondences.

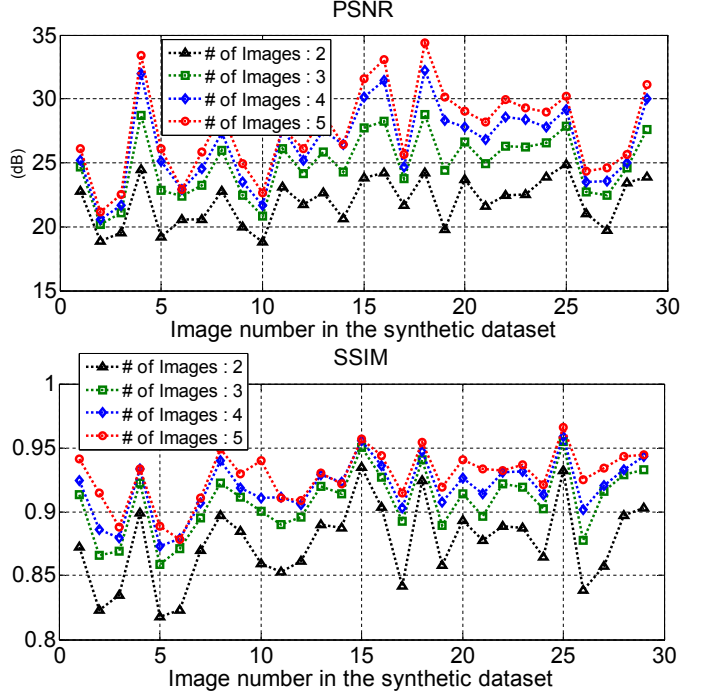


Fig. 8. The performance variations of the proposed method according to the number of fluttering patterns used.

As shown in Fig. 7(f), our algorithm shows a promising result of moving object deblurring in a complex background. The refinement is iterated 2 or 3 times for the final result and takes 5 minutes for an image with 800×600 resolution in our MATLAB implementation. Of that time, the computation on GMM takes 1 minute, trimaps and matting take 1 minute, and PSF estimation and deblurring take 1 minute in the initialization step. In the iterative refinement step, alignment with optimization in Eq. (14) takes 20 seconds, and multi-image deblurring takes 30 seconds.

We empirically set $\{\lambda_d, \lambda_a, \tau_{color}, \tau_{grad}\} = \{0.01, 0.5, 0.3, 0.5\}$. The soft constraint in Eq. (13) indicates that α is consistent with foreground pixels, so we adjust λ_m according to a blur size. We set λ_m to 0.05 if a blur size is smaller than 30 pixels, or 0.1 if otherwise.

V. EXPERIMENTS

To verify the effectiveness of the proposed method, we perform both quantitative and qualitative comparisons with other computational imaging methods; the coded exposure imaging [1] and the varying exposure video [12]. For the coded exposure method [1], we use a fluttering pattern of length 48 generated by the author's code³. The exposure sequences [30, 35, 42ms] stated in [12] is used for the varying exposure method. The fluttering patterns of length 48 of the proposed method is generated by applying Eq. (10) once to the initial set⁴.

³www.umiacs.umd.edu/~aagrawal/MotionBlur/SearchBestSeq.zip

⁴The initial set we used in this work is [000010100100; 001001111101; 101000100011; 001110010111]

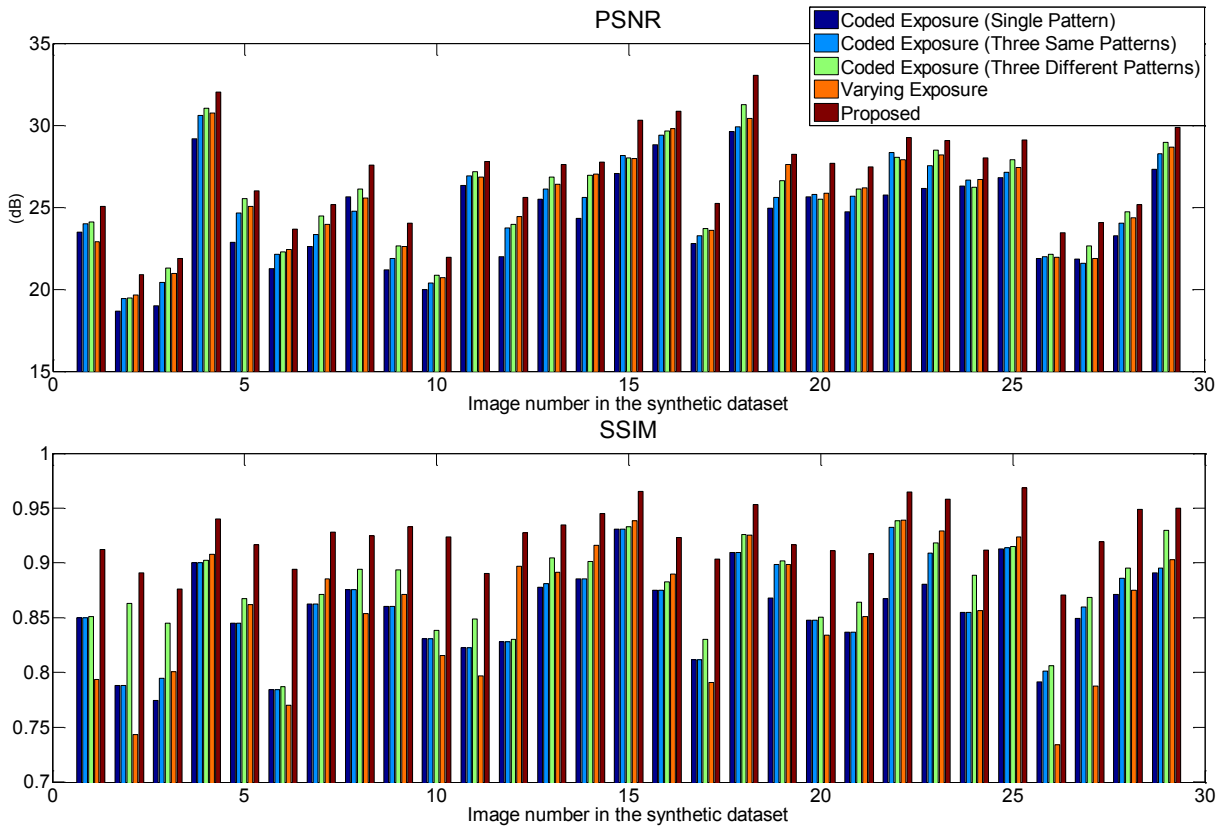


Fig. 9. The quantitative comparisons of different methods on image deblurring.

We also perform comparisons with state-of-the-art deblurring algorithms [50], [51], [52], [53]. By comparing the proposed method with the deblurring algorithms, we demonstrate the synergy between our hardware configuration and software algorithm over the conventional software-based approaches. In the recent benchmark for single image blind deblurring [54], two-phase kernel estimation method [50] achieves the best result with large motion blur in the presence of noise. Deblurring with a dark channel prior [51] also shows superior performance over other single image deblurring methods. The researches in [52], [53] propose video deblurring algorithms which jointly estimate object segmentation and camera motion where each layer can be deblurred well. We obtain the results of [50], [51], [52] by running the codes released by authors⁵. The result of [53] are provided by the author.

A. Synthetic Experiments

For quantitative evaluations, we perform synthetic experiments. As the synthetic data, we use 29 images downloaded from Kodak Lossless True Color Image Suite [55]. Image blur is simulated by the 1D filtering with different exposure sequences generated by each method. To simulate a real photography, we add the intensity dependent Gaussian noise with the standard deviation $\sigma = 0.01\sqrt{i}$ where i is the noise-free intensity of the blurred images in $[0, 1]$ [56]. The

⁵[50]: http://www.cse.cuhk.edu.hk/leojia/projects/robust_deblur/index.html
[51]: <http://vllab1.ucmerced.edu/~jinshan/projects/dark-channel-deblur/>
[52]: <http://cv.snu.ac.kr/research/~VD/>

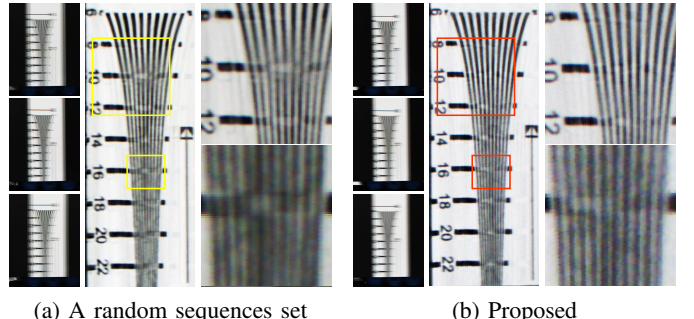


Fig. 10. Comparison of results using a random set and the proposed complementary set when PSFs are stretched (Blur size : 96 pixels).

peak signal-to-noise ratio (PSNR) and the gray-scale structural similarity (SSIM) [57] are used as the quality metrics. For fair comparisons, we conduct parameter sweeps for image deblurring and the highest PSNR and SSIM values of each image/method are reported.

Fig. 8 reports the averaged PSNR and SSIM of the proposed method according to the number of images used. We can observe that better performance is achieved with more images, however, the performance gain ratio is reduced as the number of images increases. The experiment shows that utilizing three fluttering patterns is a good trade-off between the performance gain and the burden of multi-image deblurring for the proposed method. Therefore we use three fluttering patterns for the remaining experiments.

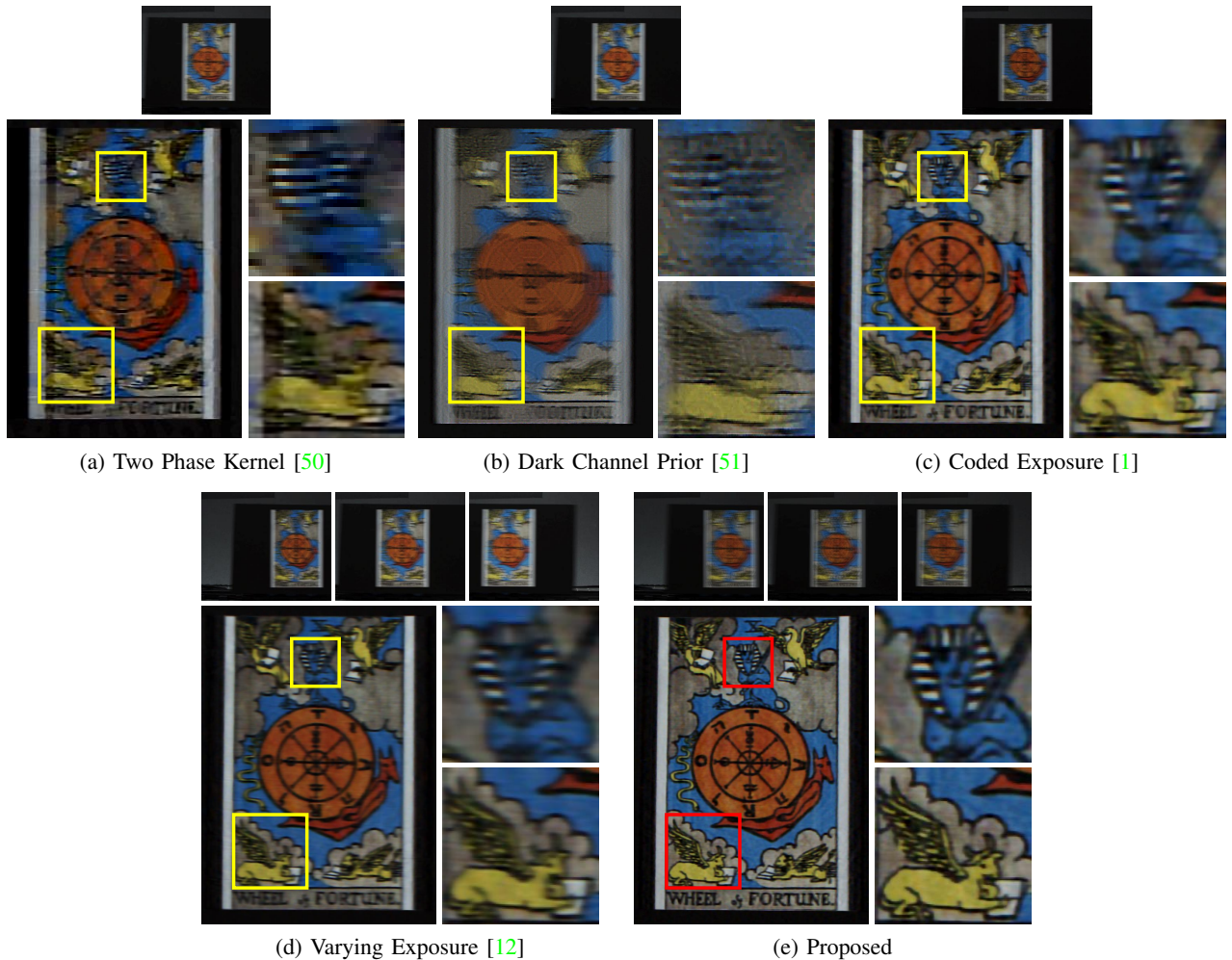


Fig. 11. Indoor experiment. A static camera is used for taking the fast moving object.

Quantitative comparisons of different methods are shown in Fig. 9. For a complete verification, we additionally consider two sets of coded exposure sequences generated by the random sample search [1]. Each set of three sequences consists of the same fluttering pattern and three different patterns, respectively. We include this two sets of sequences as baseline extensions of a single coded exposure to coded exposure video. Although deblurred images from the same fluttering pattern will have almost same results each other, we can expect an effect of a mean filter that suppresses deconvolution noise. The proposed method outperforms the previous methods for all the dataset, with large margins especially in SSIM. This is because the proposed method yields high-quality deblurring results while the previous methods fail to recover textured regions due to the loss of high spatial frequencies. Fig. 1 shows examples of the synthetic result. As shown in the figures, our method outperforms the other methods both qualitatively and quantitatively.

B. Real-world Experiments

In Fig. 10, we show an empirical validation of the performance issue related to the object velocity, discussed in Sec. III-B. We captured a resolution chart in a carefully

controlled environment as shown in Fig. 4. We let the chart move along a straight track at a constant speed. In the captured images, the chart moved two pixels during one exposure chop. We compare our complementary set with a set of randomly generated fluttering patterns. As shown in Fig. 10, when PSF is stretched twice, the deblurred image captured by the random sequence set has noticeable artifacts around edges. On the other hand, the proposed complementary set is able to preserve the details on the resolution chart.

Fig. 11 compares the results from the images captured in an indoor environment. Earlier, we explained that traditional exposure destroys spatial frequencies of the blurred image. Software-based deblurring algorithms [50], [51] fail to recover a clean image due to the frequency loss even though they use well-designed priors and perform post processing. The proposed method yields a sharper image and recovers details better than the other methods.

We further apply our coded exposure video framework to a robotics application. Handling motion blur is critical for robotics applications such as visual odometry and SLAM [58] as the blur can significantly degrade their performance. We attached our coded exposure video system to a wheeled robot as shown in Fig. 12, where the speed of the robot is about

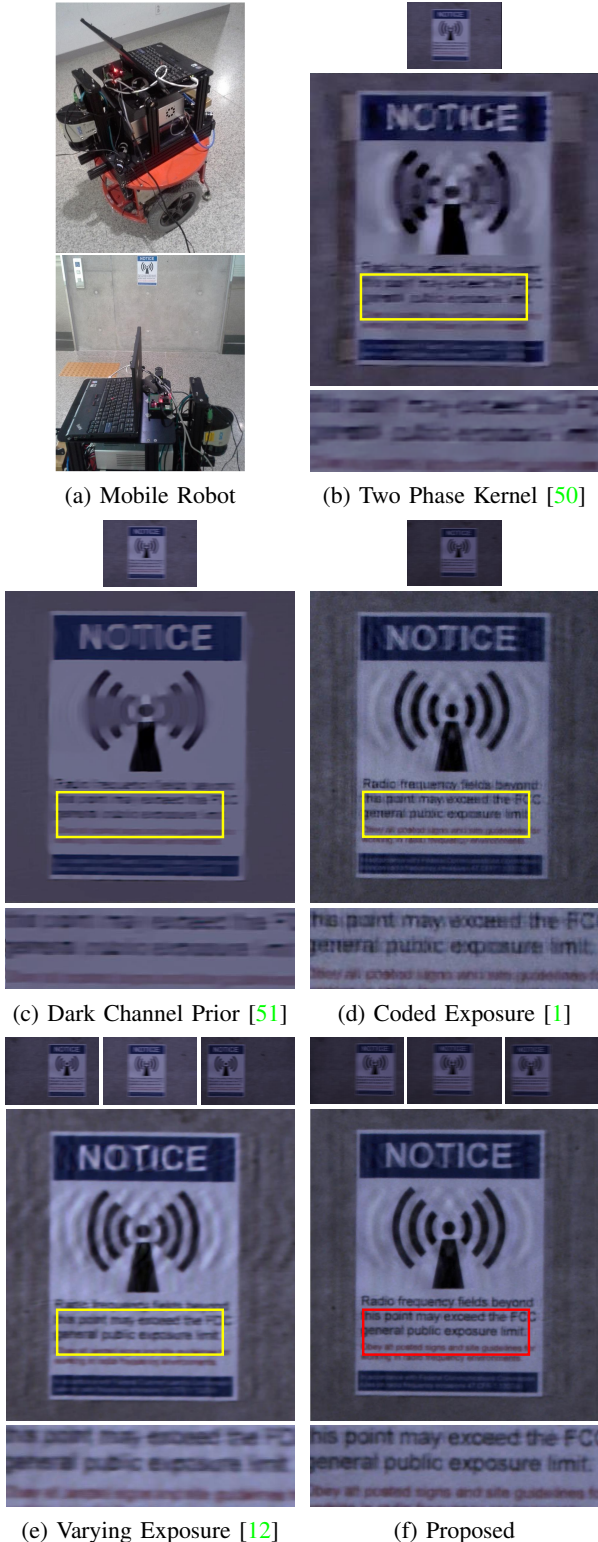


Fig. 12. Mobile robot application. The robot captures image sequentially using a side-view camera.

1 meter per second. As shown in Fig. 12, using the coded exposure video enables the recovery of sharp images compared to the other methods. Note that the ringing artifacts in the results are caused by the violations of the constant velocity and the linear motion assumptions.

Fig. 13 shows the results of deblurring multiple objects with different velocities. To segment each object trimap separately, we performed multi-label optimization via graph-cuts [59]. Then, each object was deblurred and pasted onto the background independently. In Fig. 13, one object is highly textured and moving fast, while the other one is lowly textured and moving slow. We compare our result to video deblurring methods in [52], [53]. Pixel-wise blur kernels using optical flow [52] are estimated at each frame. Although these methods segment foreground blurred objects successfully, the deblurred image is still blurry. The proposed method shows the best result compared to the other methods including computational imaging approaches [1], [12].

We then perform another real-world experiment in outdoor by capturing a fast moving object as shown in Fig. 14. The motion direction and the blur kernel is estimated automatically in the complex background that has a similar color as the moving car. Software-based approaches [52], [53] fail to compute latent images. In [52], image restoration quality depends on the performance of optical flow. Complex background structure results in the inaccurate estimation of optical flow and blur kernels. The result of [53] shows a relatively good deblurred image because a user-defined soft segmentation helps extract a blurred foreground object, however, texts and edges in the deblurred image are not recovered accurately. On the other hand, computational imaging methods show good performance. In particular, our coded exposure video scheme outperforms all the other methods [1], [12].

VI. APPLICATION TO A PRIVACY PROTECTION METHOD FOR VIDEO SURVEILLANCE

The privacy protection for video surveillance has become an important issue recently as the video surveillance has become a commonplace. Various attempts have been made to address the issue in computer vision [61], [62], [63] and an interesting study is the use of a coprime blur scheme, which strategically blurs surveillance videos for privacy protection [14].

The coprime blur scheme encrypts video streams by applying two different blur kernels which satisfy *coprimality*, and forms a public stream and a private stream. An unblurred stream can be recovered by a coprime deblurring algorithm when both the private and public streams can be accessed. Since it is very difficult to apply blind deconvolution with only a public stream, the privacy in video streams is protected and a higher level of security can be achieved by choosing different blur kernels for each frame. In [14], Li *et al.* synthesized the coprime blur kernels from two binary sequences and presented an efficient deblurring algorithm. They also highlighted the importance of constructing a bank of blur kernels with flat spectrum because it directly affects the security-level and the quality of recovered videos.

Our complementary sets of fluttering patterns can be directly applied to design the coprime blur kernels in the same manner⁶. Because we can generate diverse sets of fluttering

⁶According to [64], two different sequences are generally coprime. To verify the coprimality of complementary pairs of sequences, we generated 120 complementary pairs of sequences of length 256 and confirmed that all the pairs satisfy the coprimality by Euclid's algorithm [65].

TABLE II

QUANTITATIVE COMPARISON OF THE COPRIME BLUR SCHEME ON THE CAVIAR DATASET. WE COMPARE THE RESULTS FROM THE RANDOM SETS, MURA [60], AND THE PROPOSED COMPLEMENTARY SETS USING THE SSIM MEASURE (MINIMUM / MAXIMUM / AVERAGE).

Dataset (# of frames)	WalkByShop1front (2360)	WalkByShop1cor (2360)	Meet WalkTogether1 (700)	TwoLeaveShop1front (1343)
Random sets	0.0000 / 1.0000 / 0.9786	0.3478 / 1.0000 / 0.9885	0.1504 / 0.9999 / 0.7054	0.1572 / 1.0000 / 0.9475
MURA [60]	0.2233 / 1.0000 / 0.9762	0.6460 / 1.0000 / 0.9899	0.0934 / 0.9998 / 0.4988	0.1870 / 1.0000 / 0.9307
Proposed	0.9793 / 1.0000 / 0.9989	0.9419 / 1.0000 / 0.9991	0.9817 / 0.9999 / 0.9873	0.9514 / 1.0000 / 0.9813

patterns with various lengths and flat spectrum, our method is suitable to achieve both high-level security and high-quality recovery.

We performed experiments to show the effectiveness of our framework applied to the coprime blur scheme. We first generate a pair of coprime blur kernel by using the modified uniformly redundant array (MURA) [60], and ten pairs of coprime blur kernels by using the random sample search [1] and our complementary sequences. Then, we encrypt the video⁷ by synthetically blurring each frame and decrypt it according to the coprime method in [14]⁸. We report the statistics of SSIM values on various datasets in Table II.

As an example, both the encryption and the decryption results by the coprime method are shown in Fig. 15. The odd rows represent encrypted frames with coprime blur kernels and the even rows show the deblurred results. The coprime method consistently produces high-quality reconstruction results with our complementary sequences while it suffers from severe artifacts in some cases when other sequences are used. This is because the random sample search fails to generate good sequences with long length due to the large search space as discussed in [2] and the MURA includes deep dips that result in spectral leakage as shown in [1]. On the other hand, our complementary sequences are able to produce good sequence pairs with various length and sets.

VII. DISCUSSION

In this paper, we presented a novel coded exposure framework for multi-image deblurring based on the new concept of complementary sets of fluttering patterns. The proposed method preserves all frequencies in the blurring process by applying different shutter patterns at each frame. Our work essentially combines the coded exposure imaging and the varying exposure video, taking advantages of the two methods to yield superior deblurring results. The effectiveness of the proposed framework has been demonstrated by both the theoretical analysis of the optimal boundaries and many experiments. Our complementary sets can also be applied to the video privacy protection for video surveillance as well as motion deblurring.

One limitation of the proposed method is the difficulty of the hardware implementation. Our method requires a machine vision camera supporting a trigger mode 5, while the varying exposure video method [12] can work with an auto exposure bracketing mode in consumer DSLR cameras. However, we have shown that our method achieves a big improvement in

terms of SNR in deblurring images over other methods. The proposed framework can be applicable for defect detection in a manufacturing system and event detection in a surveillance system where there is inevitable large motion blur due to a high-speed conveyor belt and fast moving objects. We also expect that new commercial cameras equipped with a high-speed global shutter [66], [67] will ease the implementation of our framework in the near future.

Another limitation is that we only solve for a 1D linear blur of a constant velocity object. Although many object motions such as a walking person or a moving car result in 1D motion blur as mentioned in [1], [68], more general PSF estimation such as spatially varying blur will be a promising direction in the future.

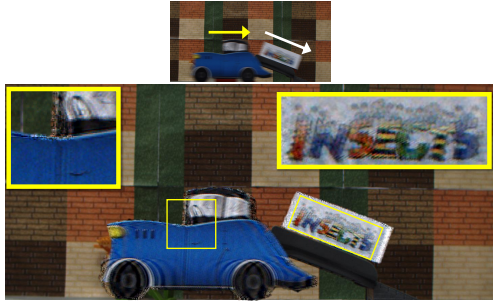
As the future work, we would like to explore further applications of the proposed framework such as multi-image super-resolution and robotics applications. It has been shown that a higher resolution image can be recovered from blurred image sequences [69], [70] and we can potentially enhance the resolution of the deblurred image from our flutter shutter camera. We also believe that the proposed system can improve the performance of a robot vision system that needs to restore blurry images due to rapid motion [52].

REFERENCES

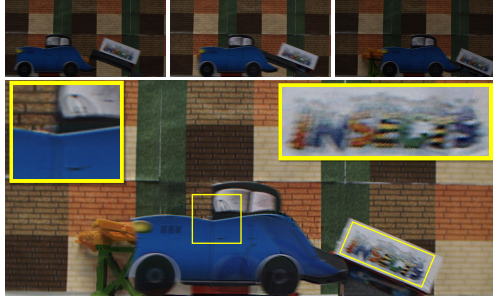
- [1] R. Raskar, A. Agrawal, and J. Tumblin, "Coded exposure photography: motion deblurring using fluttered shutter," *ACM Transactions on Graphics*, vol. 25, no. 3, pp. 795–804, 2006.
- [2] H.-G. Jeon, J.-Y. Lee, Y. Han, S. J. Kim, and I. S. Kweon, "Fluttering pattern generation using modified Legendre sequence for coded exposure imaging," in *Proceedings of IEEE International Conference on Computer Vision (ICCV)*, 2013.
- [3] S. McCloskey, Y. Ding, and J. Yu, "Design and estimation of coded exposure point spread functions," *IEEE Transactions on Pattern Analysis and Machine Intelligence (PAMI)*, vol. 34, no. 10, pp. 2071–2077, 2012.
- [4] S. McCloskey, W. Au, and J. Jelinek, "Iris capture from moving subjects using a fluttering shutter," in *IEEE International Conference on Biometrics: Theory Applications and Systems (BTAS)*, 2010.
- [5] W. Xu and S. McCloskey, "2d barcode localization and motion deblurring using a flutter shutter camera," in *IEEE Workshop on Applications of Computer Vision (WACV)*, 2011.
- [6] S. S. Gorthi, D. Schaak, and E. Schonbrun, "Fluorescence imaging of flowing cells using a temporally coded excitation," *Optics Express*, vol. 21, no. 4, pp. 5164–5170, 2013.
- [7] C. Ma, Z. Liu, L. Tian, Q. Dai, and L. Waller, "Motion deblurring with temporally coded illumination in an led array microscope," *Optics Letters*, vol. 40, no. 10, pp. 2281–2284, 2015.
- [8] Y. Tendero, J.-M. Morel, and B. Rougé, "The flutter shutter paradox," *SIAM Journal on Imaging Sciences*, vol. 6, no. 2, pp. 813–847, 2013.
- [9] L. Zhang, A. Deshpande, and X. Chen, "Denoising vs. deblurring: Hdr imaging techniques using moving cameras," in *Proceedings of IEEE Conference on Computer Vision and Pattern Recognition (CVPR)*, 2010.
- [10] G. Boracchi and A. Foi, "Modeling the performance of image restoration from motion blur," *IEEE Transactions on Image Processing (TIP)*, vol. 21, no. 8, pp. 3502–3517, 2012.
- [11] S. Park and M. Levoy, "Gyro-based multi-image deconvolution for removing handshake blur," in *Proceedings of IEEE Conference on Computer Vision and Pattern Recognition (CVPR)*, 2014.

⁷dataset: <http://homepages.inf.ed.ac.uk/rbf/CAVIAR/>

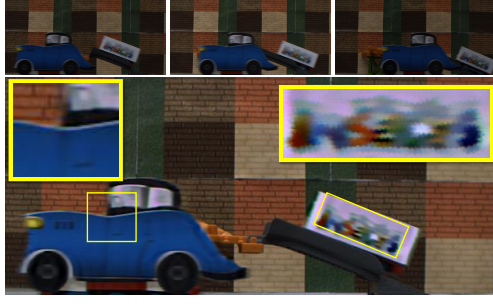
⁸We used the deblurring code by the author to decrypt the video - <http://fengl.org/publications/>



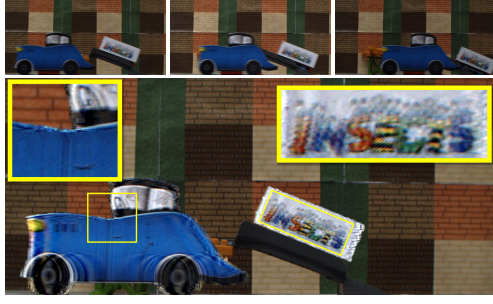
(a) Coded Exposure [1]



(b) Pixel-wise Blur Estimation [52]



(c) Soft Segmentation [53]



(d) Varying Exposure [12]

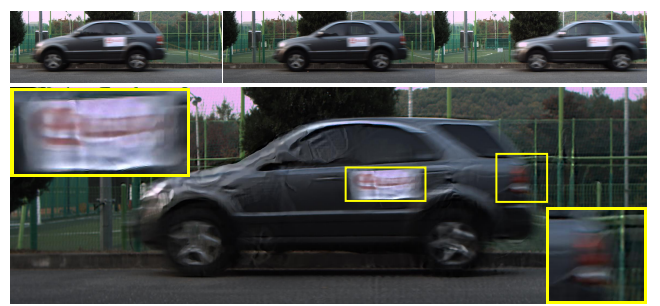


(e) Proposed

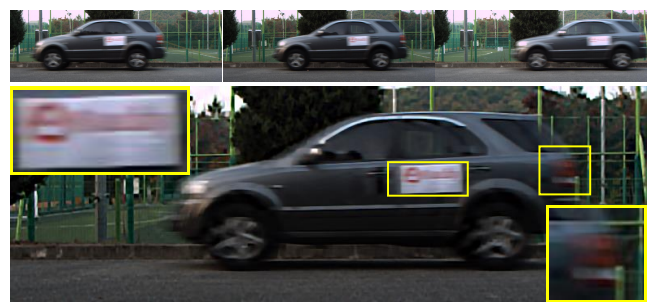
Fig. 13. Multiple objects deblurring with different velocities and directions. Blur size of the car (close) and the panel (far) (unit: pixel): (a) 50 and 45. (b,c,d) [36 44 39] and [25 31 27]. (e) [46 50 52] and [35 38 44].



(a) Coded Exposure [1]



(b) Pixel-wise Blur Estimation [52]



(c) Soft Segmentation [53]



(d) Varying Exposure [12]



(e) Proposed

Fig. 14. Outdoor Experiment. Blur size of the car (close) and the panel (far) (unit: pixel): (a) 80. (b,c,d) [60 67 75]. (e) [80 80 82].



Fig. 15. Coprime blur scheme for the privacy-protection in video surveillance. We show both the encrypted (top) and the decrypted (bottom) frames (1652, 1856, 1946, 2193 from the left to right) of the “WalkByShop1front” video.

- [12] A. Agrawal, Y. Xu, and R. Raskar, “Invertible motion blur in video,” in *Proceedings of ACM SIGGRAPH*, 2009.
- [13] H.-G. Jeon, J.-Y. Lee, Y. Han, S. J. Kim, and I. S. Kweon, “Complementary sets of shutter sequences for motion deblurring,” in *Proceedings of IEEE International Conference on Computer Vision (ICCV)*, 2015.
- [14] F. Li, Z. Li, D. Saunders, and J. Yu, “A theory of coprime blurred pairs,” in *Proceedings of IEEE International Conference on Computer Vision (ICCV)*, 2011.
- [15] W. H. Richardson, “Bayesian-based iterative method of image restoration,” *Journal of the Optical Society of America*, vol. 62, pp. 55–59, 1972.
- [16] L. B. Lucy, “An iterative technique for the rectification of observed distributions,” *Astronomical Journal*, vol. 79, pp. 745–754, 1974.
- [17] N. Wiener, *Extrapolation, Interpolation, and Smoothing of Stationary Time Series*. The MIT Press, 1964.
- [18] L. Yuan, J. Sun, L. Quan, and H.-Y. Shum, “Image deblurring with blurred/noisy image pairs,” *ACM Transactions on Graphics*, vol. 26, no. 3, 2007.
- [19] J.-F. Cai, H. Ji, C. Liu, and Z. Shen, “Blind motion deblurring using multiple images.” *Journal of Computational Physics*, vol. 228, no. 14, pp. 5057–5071, 2009.
- [20] J. Chen, L. Yuan, C. keung Tang, and L. Quan, “Robust dual motion deblurring,” in *Proceedings of IEEE Conference on Computer Vision and Pattern Recognition (CVPR)*, 2008.
- [21] S. Cho, J. Wang, and S. Lee, “Video deblurring for hand-held cameras using patch-based synthesis,” *ACM Transactions on Graphics*, vol. 31, no. 4, pp. 64:1–64:9, 2012.
- [22] M. Delbracio and G. Sapiro, “Burst deblurring: Removing camera shake through fourier burst accumulation,” in *Proceedings of IEEE Conference on Computer Vision and Pattern Recognition (CVPR)*, 2015.
- [23] O. Shahar, A. Faktor, and M. Irani, “Space-time super-resolution from a single video,” in *Proceedings of IEEE Conference on Computer Vision and Pattern Recognition (CVPR)*, 2011.
- [24] E. Shechtman, Y. Caspi, and M. Irani, “Space-time super-resolution,” *IEEE Transactions on Pattern Analysis and Machine Intelligence (PAMI)*, vol. 27, no. 4, pp. 531–545, 2005.

- [25] K. Sato, S. Ishizuka, A. Nikami, and M. Sato, "Control techniques for optical image stabilizing system," *IEEE transactions on Consumer Electronics*, vol. 39, no. 3, pp. 461–466, 1993.
- [26] R. Chereau and T. P. Breckon, "Robust motion filtering as an enabler to video stabilization for a tele-operated mobile robot," in *SPIE Security+ Defence*, 2013.
- [27] P. Llull, X. Liao, X. Yuan, J. Yang, D. Kittle, L. Carin, G. Sapiro, and D. J. Brady, "Coded aperture compressive temporal imaging," *Optics Express*, vol. 21, no. 9, pp. 10 526–10 545, 2013.
- [28] D. Liu, J. Gu, Y. Hitomi, M. Gupta, T. Mitsunaga, and S. Nayar, "Efficient space-time sampling with pixel-wise coded exposure for high speed imaging," *IEEE Transactions on Pattern Analysis and Machine Intelligence (PAMI)*, vol. 36, no. 2, pp. 248–260, 2014.
- [29] D. Reddy, A. Veeraraghavan, and R. Chellappa, "P2C2: Programmable pixel compressive camera for high speed imaging," in *Proceedings of IEEE Conference on Computer Vision and Pattern Recognition (CVPR)*, 2011.
- [30] S. McCloskey, "Temporally coded flash illumination for motion deblurring," in *Proceedings of IEEE International Conference on Computer Vision (ICCV)*, 2011.
- [31] J. Holloway, A. C. Sankaranarayanan, A. Veeraraghavan, and S. Tambe, "Flutter shutter video camera for compressive sensing of videos," in *Proceedings of IEEE International Conference on Computational Photography (ICCP)*, 2012.
- [32] H.-G. Jeon, J.-Y. Lee, Y. Han, S. J. Kim, and I. S. Kweon, "Generating fluttering pattern with low autocorrelation for coded exposure imaging," *International Journal of Computer Vision (IJCV)*, pp. 1–18, 2016.
- [33] C.-C. Tseng and C. L. Liu, "Complementary sets of sequences," *IEEE Transactions on Information Theory*, vol. 18, no. 5, pp. 644–652, 1972.
- [34] C. Cook, *Radar signals: An introduction to theory and application*. Elsevier, 2012.
- [35] P. Spasojevic and C. N. Georghiades, "Complementary sequences for ISI channel estimation," *IEEE Transactions on Information Theory*, vol. 47, no. 3, pp. 1145–1152, 2001.
- [36] J. M. Jensen, H. E. Jensen, and T. Høholdt, "The merit factor of binary sequences related to difference sets," *IEEE Transactions on Information Theory*, vol. 37, no. 3, pp. 617–626, 1991.
- [37] A. Ukil, "Low autocorrelation binary sequences: Number theory-based analysis for minimum energy level, barker codes," *Digital Signal Processing*, vol. 20, no. 2, pp. 483–495, 2010.
- [38] M. Soltanianian, M. M. Naghsh, and P. Stoica, "A fast algorithm for designing complementary sets of sequences," *Signal Processing*, vol. 93, no. 7, pp. 2096–2102, 2013.
- [39] S. McCloskey, "Velocity-dependent shutter sequences for motion deblurring," in *Proceedings of European Conference on Computer Vision (ECCV)*, 2010.
- [40] M. G. Parker, K. G. Paterson, and C. Tellambura, *Golay Complementary Sequences*. In Wiley Encyclopedia of Telecommunications, 2003.
- [41] P. Fan, N. Suehiro, N. Kuroyanagi, and X. Deng, "Class of binary sequences with zero correlation zone," in *Electronics Letters*, vol. 35, no. 10, 1999, pp. 777–779.
- [42] A. Agrawal and Y. Xu, "Coded exposure deblurring: Optimized codes for PSF estimation and invertibility," in *Proceedings of IEEE Conference on Computer Vision and Pattern Recognition (CVPR)*, 2009.
- [43] S. Dai and Y. Wu, "Motion from blur," in *Proceedings of IEEE Conference on Computer Vision and Pattern Recognition (CVPR)*, 2008.
- [44] Y.-W. Tai, N. Kong, S. Lin, and S. Y. Shin, "Coded exposure imaging for projective motion deblurring," in *Proceedings of IEEE Conference on Computer Vision and Pattern Recognition (CVPR)*, 2010.
- [45] A. Levin, D. Lischinski, and Y. Weiss, "A closed-form solution to natural image matting," *IEEE Transactions on Pattern Analysis and Machine Intelligence (PAMI)*, vol. 30, no. 2, pp. 228–242, 2008.
- [46] D. G. Lowe, "Distinctive image features from scale-invariant keypoints," *International Journal of Computer Vision (IJCV)*, vol. 60, no. 2, pp. 91–110, 2004.
- [47] J.-Y. Lee, Y. Matsushita, B. Shi, I. S. Kweon, and K. Ikeuchi, "Radiometric calibration by rank minimization," *IEEE Transactions on Pattern Analysis and Machine Intelligence (PAMI)*, vol. 35, no. 1, pp. 144–156, 2013.
- [48] A. Levin, R. Fergus, F. Durand, and W. T. Freeman, "Image and depth from a conventional camera with a coded aperture," *ACM Transactions on Graphics*, vol. 26, no. 3, 2007.
- [49] S. Kim, Y.-W. Tai, Y. Bok, H. Kim, and I. S. Kweon, "Two-phase approach for multi-view object extraction," in *Proceedings of International Conference on Image Processing (ICIP)*, 2011.
- [50] L. Xu and J. Jia, "Two-phase kernel estimation for robust motion deblurring," in *Proceedings of European Conference on Computer Vision (ECCV)*, 2010.
- [51] J. Pan, D. Sun, H. Pfister, and M.-H. Yang, "Blind image deblurring using dark channel prior," 2016.
- [52] T. H. Kim and K. M. Lee, "Generalized video deblurring for dynamic scenes," in *Proceedings of IEEE Conference on Computer Vision and Pattern Recognition (CVPR)*, 2015.
- [53] J. Pan, Z. Hu, Z. Su, H.-Y. Lee, and M.-H. Yang, "Soft-segmentation guided object motion deblurring," 2016.
- [54] W.-S. Lai, J.-B. Huang, Z. Hu, N. Ahuja, and M.-H. Yang, "A comparative study for single image blind deblurring," 2016.
- [55] R.W.Franzen. (1999, Jun.) Kodak lossless true color image suite. [Online]. Available: <http://www.r0k.us/graphics/kodak/>
- [56] Y. Y. Schechner, S. K. Nayar, and P. N. Belhumeur, "Multiplexing for optimal lighting," *IEEE Transactions on Pattern Analysis and Machine Intelligence (PAMI)*, vol. 29, no. 8, pp. 1339–1354, Aug 2007.
- [57] Z. Wang, A. C. Bovik, H. R. Sheikh, and E. P. Simoncelli, "Image quality assessment: from error visibility to structural similarity," *IEEE Transactions on Image Processing (TIP)*, vol. 13, no. 4, pp. 600–612, 2004.
- [58] A. S. Huang, A. Bachrach, P. Henry, M. Krainin, D. Maturana, D. Fox, and N. Roy, "Visual odometry and mapping for autonomous flight using an RGB-D camera," in *International Symposium on Robotics Research (ISRR)*, 2011.
- [59] Y. Boykov, O. Veksler, and R. Zabih, "Fast approximate energy minimization via graph cuts," *IEEE Transactions on Pattern Analysis and Machine Intelligence (PAMI)*, vol. 23, no. 11, pp. 1222–1239, 2001.
- [60] S. R. Gottesman and E. Fenimore, "New family of binary arrays for coded aperture imaging," *Applied Optics*, vol. 28, no. 20, pp. 4344–4352, 1989.
- [61] M. Upmanyu, A. M. Namboodiri, K. Srinathan, and C. Jawahar, "Efficient privacy preserving video surveillance," in *Proceedings of IEEE International Conference on Computer Vision (ICCV)*, 2009.
- [62] A. Chattopadhyay and T. E. Boult, "Privacycam: a privacy preserving camera using uclinux on the blackfin dsp," in *Proceedings of IEEE Conference on Computer Vision and Pattern Recognition (CVPR)*, 2007.
- [63] F. Pittaluga and S. J. Koppal, "Privacy preserving optics for miniature vision sensors," in *Proceedings of IEEE Conference on Computer Vision and Pattern Recognition (CVPR)*, 2015.
- [64] E. Kaltofen, Z. Yang, and L. Zhi, "On probabilistic analysis of randomization in hybrid symbolic-numeric algorithms," in *Proceedings of the international workshop on Symbolic-numeric computation*, 2007.
- [65] E. K. Donald, "The art of computer programming," *Sorting and searching*, vol. 3, pp. 426–458, 1999.
- [66] "Panasonic develops 10 times higher saturation & highly functional global shutter technology by controlling of organic-photoconductive-film on cmos image sensor," <http://news.panasonic.com/global/press/data/2016/02/en160203-6/en160203-6.html>.
- [67] "Jvc gy-hm100u," http://pro.jvc.com/prof/attributes/tech_desc.jsp?model_id=MDL101845&feature_id=02.
- [68] A. Levin, P. Sand, T. S. Cho, F. Durand, and W. T. Freeman, "Motion-invariant photography," *ACM Transactions on Graphics*, vol. 27, no. 3, pp. 71:1–71:9, 2008.
- [69] E. Faramarzi, D. Rajan, and M. P. Christensen, "Unified blind method for multi-image super-resolution and single/multi-image blur deconvolution," *IEEE Transactions on Image Processing (TIP)*, vol. 22, no. 6, pp. 2101–2114, 2013.
- [70] A. Agrawal and R. Raskar, "Resolving objects at higher resolution from a single motion-blurred image," in *Proceedings of IEEE Conference on Computer Vision and Pattern Recognition (CVPR)*, 2007.



IEEE.

Hae-Gon Jeon received the BS degree in Electrical and Electronic Engineering from Yonsei University in 2011, and the MS degree in Electrical Engineering from KAIST in 2013. From Aug. 2013 to Jan. 2015, he worked as a researcher at the Personal Plug and Play DigiCar Center. He is currently working toward the Ph.D. degree in Electrical Engineering at KAIST. His research interests include computational imaging and 3D reconstruction. He is a recipient of the Samsung HumanTech Paper Award and the Qualcomm Innovation Award. He is a student member of the



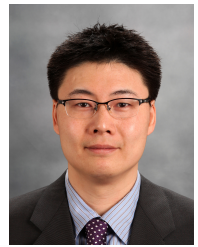
In So Kweon received the B.S. and M.S. degrees in Mechanical Design and Production Engineering from Seoul National University, Seoul, Korea, in 1981 and 1983, respectively, and the Ph.D. degree in Robotics from the Robotics Institute, Carnegie Mellon University, Pittsburgh, Pennsylvania, in 1990. He worked for the Toshiba R&D Center, Japan, and joined the Department of Automation and Design Engineering, KAIST, Seoul, Korea, in 1992, where he is now a professor with the Department of Electrical Engineering. His research interests are sensor fusion, color modeling and analysis, visual tracking, and visual SLAM. He was the general chair for the Asian Conference on Computer Vision 2012 and he is on the honorary board of the International Journal of Computer Vision (IJCV). He has been serving as a director for the Personal Plug and Play DigiCar Center which is one of the National Core Research Center since 2010. He was a member of ‘Team KAIST’ which won the first place in DARPA Robotics Challenge Finals 2015.



Joon-Young Lee received the B.S degree in Electrical and Electronic Engineering from Yonsei University, Korea in 2008. He received the M.S and Ph.D degrees in Electrical Engineering from KAIST, Korea in 2009 and 2015, respectively. He is a research scientist at Adobe Research. His research interests include deep learning, computer vision, and computational photography. He is a member of the IEEE.



Yudeog Han received the B.S degree in Electronics Engineering from Soongsil University in 2011, and the M.S degree in Division of Future Vehicle from KAIST in 2013. He joined Agency for Defense Development in 2013. He is a recipient of the Samsung HumanTech Paper Award and the Qualcomm Innovation Award. His research interests include computational photography and 3D reconstruction.



Seon Joo Kim received the BS and MS degrees from Yonsei University, Seoul, Korea, in 1997 and 2001. He received the PhD degree in computer science from the University of North Carolina at Chapel Hill in 2008. He is an assistant professor at the Department of Computer Science, Yonsei University since March 2013. His research interests include computer vision, computer graphics/computational photography, and HCI/visualization. He is a member of the IEEE.